

X-641-68-314

PREPRINT

NASA TM X-63303

AN INTEGRATED EXPERIMENT FOR COMPOSITIONAL ANALYSIS FROM AN ORBITER



ISADORE ADLER
JACOB TROMBKA

GPO PRICE \$ _____

CFSTI PRICE(S) \$ _____

Hard copy (HC) _ -

Microfiche (MF) _ -

ff 653 July 65

AUGUST 1968



GODDARD SPACE FLIGHT CENTER

GREENBELT, MARYLAND

FACILITY FORM 602

N 68-31887
(ACCESSION NUMBER)

94
(PAGES)

TMX-63303
(NASA CR OR TMX OR AD NUMBER)

(THRU)

30
(CODE)

(CATEGORY)



X-641-68-314
PREPRINT

AN INTEGRATED EXPERIMENT FOR COMPOSITIONAL
ANALYSIS FROM AN ORBITER


Isidore Adler and Jacob Trombka

August 1968

GODDARD SPACE FLIGHT CENTER
Greenbelt, Maryland

AN INTEGRATED EXPERIMENT FOR COMPOSITIONAL
ANALYSIS FROM AN ORBITER

Isidore Adler and Jacob Trombka

It is an accepted fact that some proportion of atomic and nuclear radiation naturally emitted from the moon is characteristic of the elements that make up the lunar surface. Detection and analysis of this radiation can be used to determine chemical composition. Accordingly, an integrated experiment package for measuring gamma rays — natural and induced, secondary X-rays, alpha particle emission, and neutron albedo is described. The advantages in this approach are an economy in technology and more comprehensive data collection, leading to improved interpretation of lunar processes.

INTRODUCTION

The problems in performing compositional analysis from an orbital vehicle are admittedly complex and raise the question: "What observational phenomena yield unique solutions in terms of elemental identification and concentration?" If one examines the electromagnetic and particulate spectra, he finds a limited number of possibilities; further, if he evaluates them, it is apparent that none yields very precise results by laboratory standards. Nevertheless one can establish a hierarchy of experiments, and those at the top of the list such as the gamma-ray or X-ray experiments can provide much useful geochemical information, particularly when coupled as an integrated experiment with some additional measurements of the backgrounds and particle emission.

Why consider orbital remote sensing? We know that in the very near future the actual physical sampling of the lunar surface material will be confined to a few limited areas and, of necessity, to flat terrain at low altitudes because of mission constraints. Thus, orbital experiments become exciting because of their

extended coverage and automatic averaging over large areas of the lunar surface.

The highly successful Surveyor missions carrying the alpha back-scattering experiment¹ have already yielded compositional analyses of two maria and one highland area. The interpretation of the results places the surface material in the general range of terrestrial basalts. This is in agreement with the interpretation placed by Vinogradov *et al.*² on the gamma-ray results from the Luna X flight.

The future analysis of returned lunar samples from the early Apollo missions will give even more detailed information about the landing sites. These analyses should help make the interpretation of orbital data more meaningful, and the combined compositional data acquired should permit a more meaningful picture of the moon.

GEOCHEMICAL QUESTIONS

The present approach to understanding the moon is based entirely on terrestrial analogues. One hypothesis considers the moon, like the earth, as divided into three zones of contrasting composition — a core, mantle, and crust caused by differential phase separations. The high temperatures for this differentiation have been produced by the decay processes involving potassium-40, uranium, thorium, and their radioactive daughter products. Furthermore, these elements not only supply the energy, but also are excellent indicators of chemical differentiation. For example, acidic rocks characteristic of the earth's crust contain potassium, uranium, and thorium in concentrations approximately two orders of magnitude greater than in undifferentiated rocks.

The extent of lunar melting at any time in the moon's history is the subject of disagreement and debate. Hopefully this question can be resolved by gamma-ray measurements of the concentration of potassium-40, uranium, and thorium in the lunar surface.

If the moon is in any part differentiated then it would be of great interest to locate the undifferentiated areas as sites for future landings, since these areas offer the greatest promise of primordial material and a knowledge of the early solar

system. Also, it would be exciting to find local active regions and areas where the emanations of gases such as radon and thoron are high.

In order to accomplish some of the foregoing geochemical objectives, it is believed that an integrated radiation package in orbit about the moon will determine most efficiently and uniquely the parameters from which major elemental composition can be inferred. Thus, both instrument design and data analysis procedures are being considered at Goddard Space Flight Center in cooperation with experimenters at U.C.S.D., J.P.L., A.S. and E., and Rice. The instruments being considered are a gamma-ray spectrometer, an X-ray spectrometer, an alpha-particle detector, and a fast and thermal neutron detector.³ Fig. 1 is an outline of some of the possible results.

EXPECTED RESULTS FROM INTEGRATED EXPERIMENT

Gamma-Ray Measurement

Gamma-ray measurements will be used to determine concentrations of the naturally radioactive elements potassium-40, uranium, and thorium in the lunar surface layers in various regions. Some characteristic gamma-ray pulse height spectra of naturally occurring radioactivity in terrestrial rocks are shown in Fig. 2. In addition, calculations by Arnold⁴ and Armstrong and Alsmiller⁵ indicate that one should also observe cosmic-ray-induced, characteristic gamma-ray lines from such elements as Fe, O, Si, Ca, Mg, and possibly H. These are very significant elements. The ratios of Fe/Si, Mg/Si, and Ca/Mg are considered very important indicators for understanding and identifying the differentiation process.

Fig. 3 shows one type of detector being considered for early flights. The 3" x 3" NaI (Tl activated) cylindrical crystal has a thin mantle consisting of a scintillating plastic crystal. The mantle scintillator is optically isolated from the primary NaI (Tl) crystal, and the two detectors are used in anticoincidence. The primary detector will be capable of yielding approximately 8-percent resolution for the 0.661-Mev line of cesium-137. The plastic scintillator is used to eliminate the effect of the charged-particle cosmic-ray flux within the field of view of the detector. Neutron shields are also considered to reduce the effect of secondary-induced neutron flux.

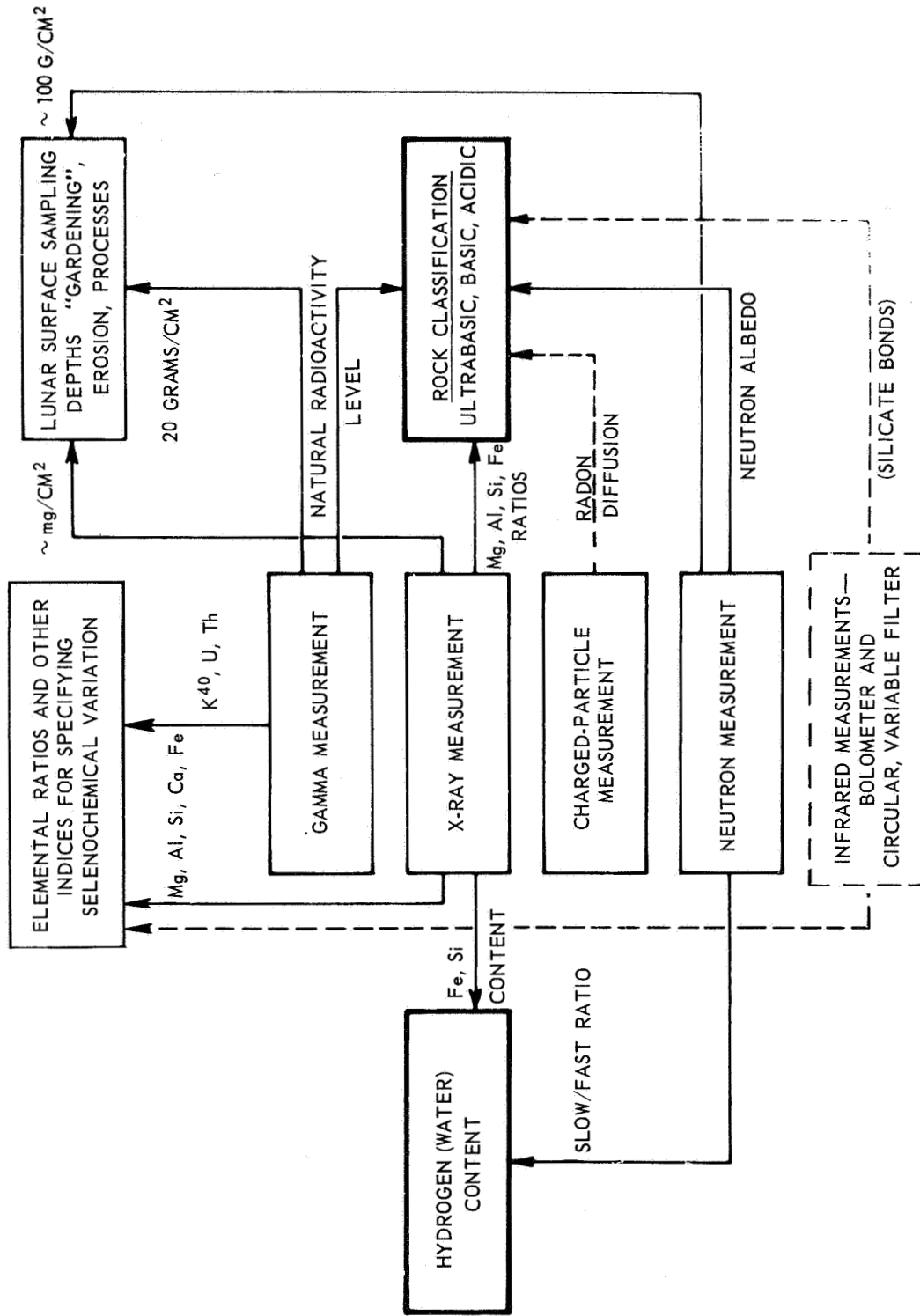


Fig. 1 Expected Results From an Integrated Radiation Detection, Remote Sensing Geochemical Experiment

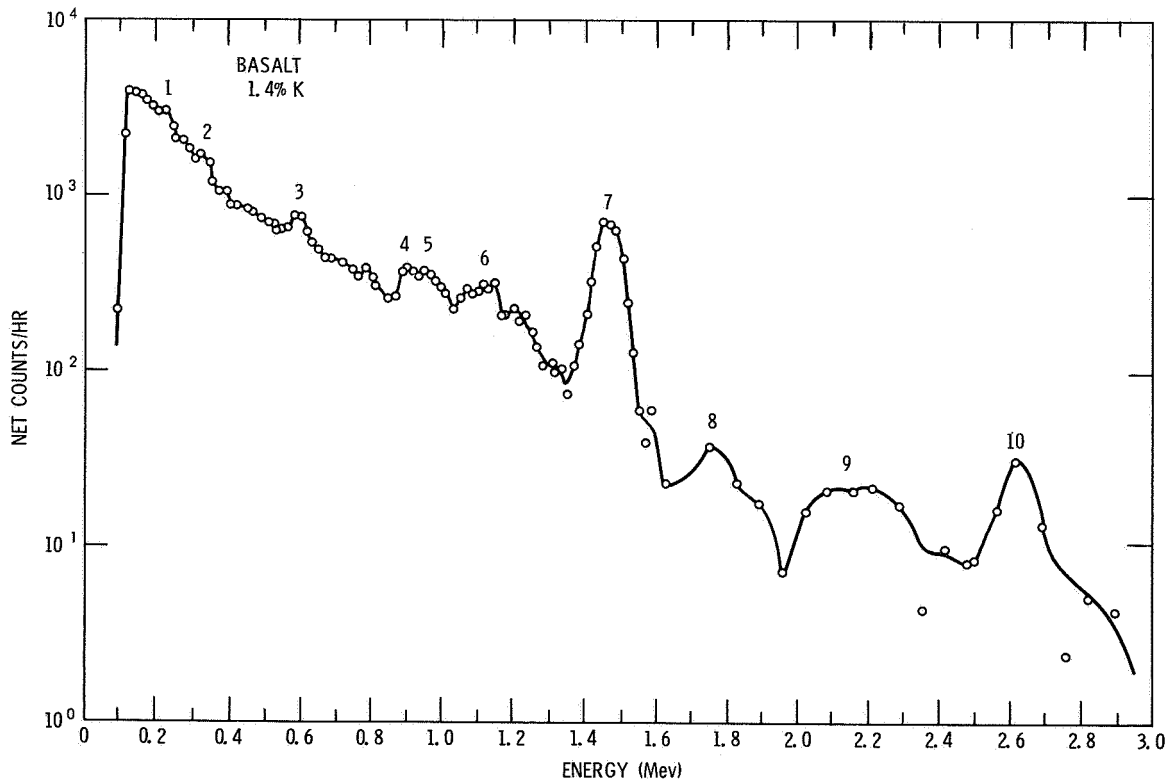
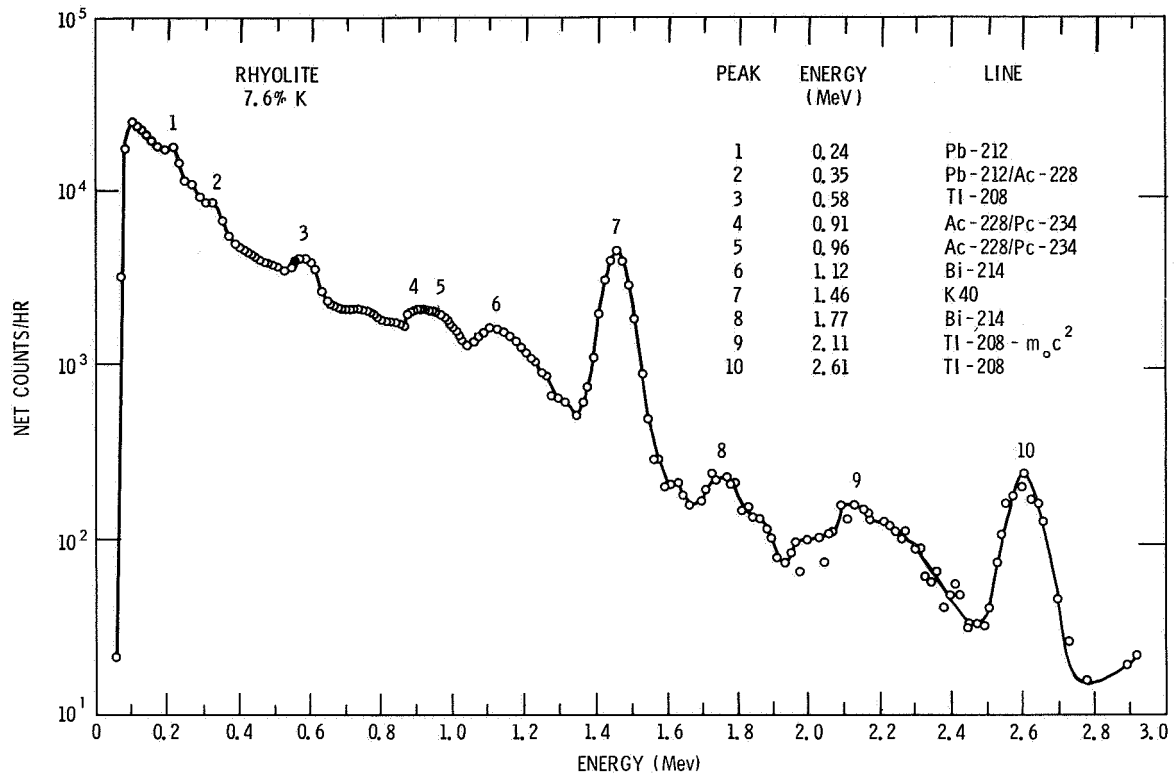


Fig. 2 Natural Radioactivity of Types of Terrestrial Rock

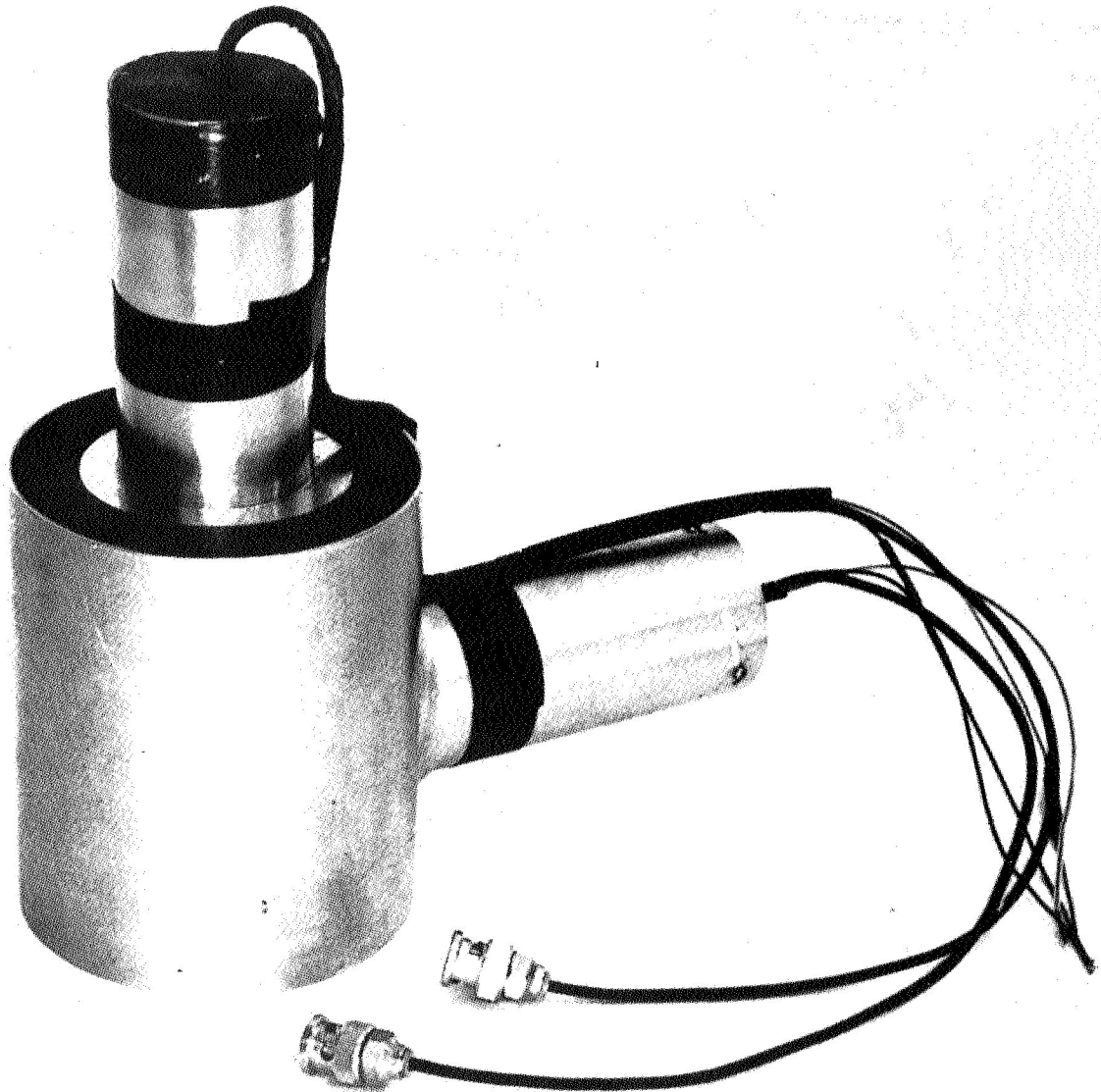


Fig. 3 Flight Prototype Scintillation Detector with Anti-Coincidence Mantle for Gamma-Ray Spectroscopy Experiment

Fig. 4 displays an engineering model of a possible flight analyzer; it is a 512-channel analyzer designed for the gamma-ray experiment and the other measurements described later. This analyzer will contain a 4096-channel memory unit and logic systems to permit its application in a multi-scaler mode as well.

X-Ray Measurement

A complementary set of measurements can be made in the soft X-ray region. Absorption of the solar X-rays by the lunar surface should give measurable

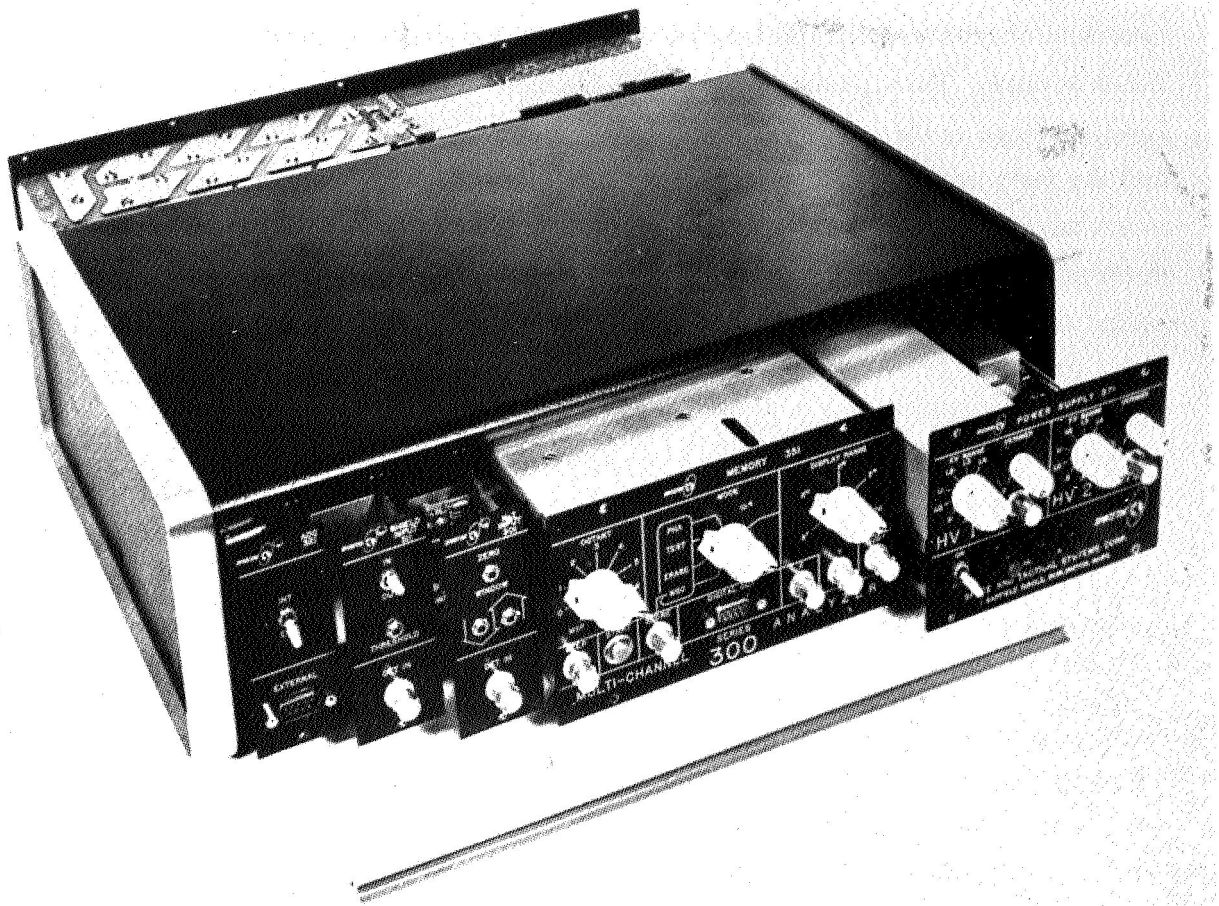


Fig. 4a Engineering Model of a Possible 512-Channel Pulse Height Analyzer

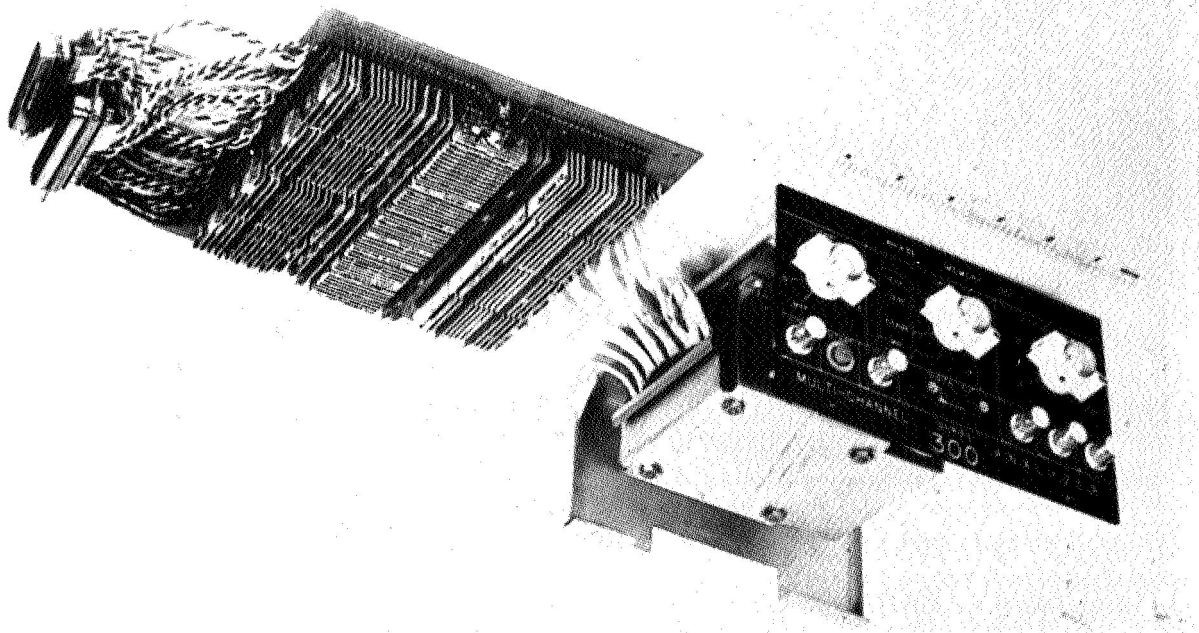


Fig. 4b View of the 4096 Memory Unit

fluxes of characteristic lines of the low atomic number elements excited by X-ray fluorescence. Thus, under normal sun conditions, one would hope to see the K-alpha lines from the more abundant elements such as O, Na, Al, Mg, and Si; and the very soft L-alpha lines from Fe, Ca, and K. One can also expect the more easily observable K-spectral lines of the Fe, Ca and K to be produced during solar flare outbursts. The results of a calculation performed by Gorenstein³ on the yield of fluorescent X-rays are shown in Table 1 for a typical basalt and a granite. The solar X-ray flux used in the computation is taken from the OSO-III daily averages for April 1967. A continuum nonflare solar flux was

Table 1

RESULTS OF A CALCULATION OF THE
YIELD OF FLUORESCENT X-RAYS

Type Rock	Element	K_{α} (Å)	Fraction by Weight	Yield of Fluorescent Photons ($\text{cm}^{-2}\text{-sec}^{-1}\text{ster}^{-1}$)
Basalt	O	23	0.38	314
	Fe(L)	17	0.14	197
	Na	11.9	0.02	24
	Mg	9.9	0.05	53
	Al	8.3	0.09	31
	Si	7.1	0.19	46
	K	3.7	0.01	0.17
	Ca	3.35	0.09	0.68
	Fe(K)	1.9	0.14	0
Granite	O		0.44	430
	Fe(L)		0.05	84
	Na		0.03	42
	Mg		0.01	7.2
	Al		0.09	34.9
	Si		0.30	82.7
	K		0.05	0.7
	Ca		0.03	0.2
	Fe(K)		0.05	0

assumed, and the spectral shape was characteristic of a free-free emission with $T = 6 \times 10^6$ °K.

Two types of detectors appear appropriate for the X-ray measurements. For radiation below 10 \AA , large-aperture, thin-window proportional counters are suitable. For the very soft X-rays, windowless detectors are under consideration. Fig. 5 is a schematic diagram of such a proportional counter. The detector would have large effective areas on the order of 100 cm^2 and Be windows of approximately .001-inch thickness. Fig. 5 shows a rotating filter wheel carrying

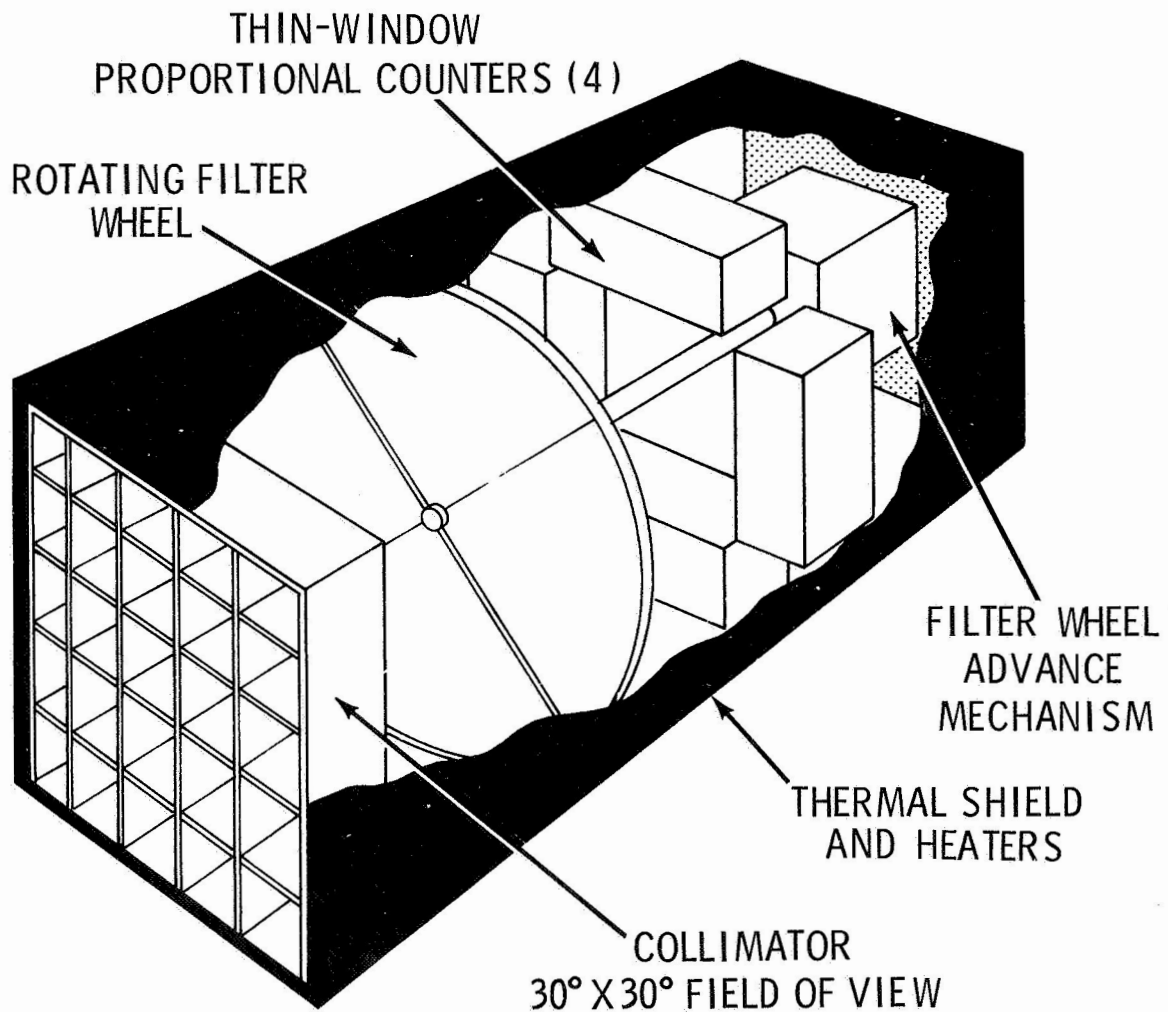


Fig. 5 Schematic of a Proportional Counter for X-ray Spectroscopy

balanced filters for energy resolution and honeycomb filters for collimation. Since the proposed counters will have good energy resolution, one can also consider using the multichannel analyzer described earlier for use in the gamma-ray experiment.

Alpha Particle Emission Measurement

There are many possible sources of alpha particle emission from the lunar surface, but perhaps the most interesting phenomenon to investigate is the diffusion of radon and thoron proposed by Kraner *et al.*⁶ They have proposed a mechanism for the diffusion of radon and thoron through the upper surface layer of the moon and the subsequent "painting" of the surface by radioactive radon and thoron decay products. Recent measurements in earth samples of radon and thoron diffusion have led to numerical estimates of the effect. Evans, Kraner, and Schroeder (see reference 3 above) measured the concentration gradients and escaping flux of radon from various types of soil in widespread regions of the United States and proposed the following model for the terrestrial process. Some portion of the radon and thoron produced by radioactive decay escapes from the host minerals into interstitial voids in the soil and then diffuses through these voids to the surface. The rate of diffusion is related to the diffusion coefficients and soil porosity. One can estimate such a process on the moon by making assumptions about composition and porosity, but he must consider other phenomena such as surface adsorption, etc. If one assumes thermal velocities for the emerging radon and thoron, then nearly all the molecules will be trapped in the moon's gravitational field. Radon, with its 3.8-day half-life, may travel a considerable distance before decaying. The thoron, on the other hand, with a 55-sec half-life would be expected to decay near its source. Both of these species would yield daughter products that conceivably could coat the surface with a varnish of active daughter products, giving characteristic spectral lines. Thus, the detection of this phenomenon could be an important indicator of active regions of emanation from the lunar surface.

The necessary equipment for the alpha particle monitoring (Fig. 6) is basically simple. The most promising detectors are solid-state, of the surface-barrier type. A mosaic of detectors providing a collection area of approximately 100 cm² is proposed. Energy resolution is provided by the use of a pulse height analyzer as described earlier.

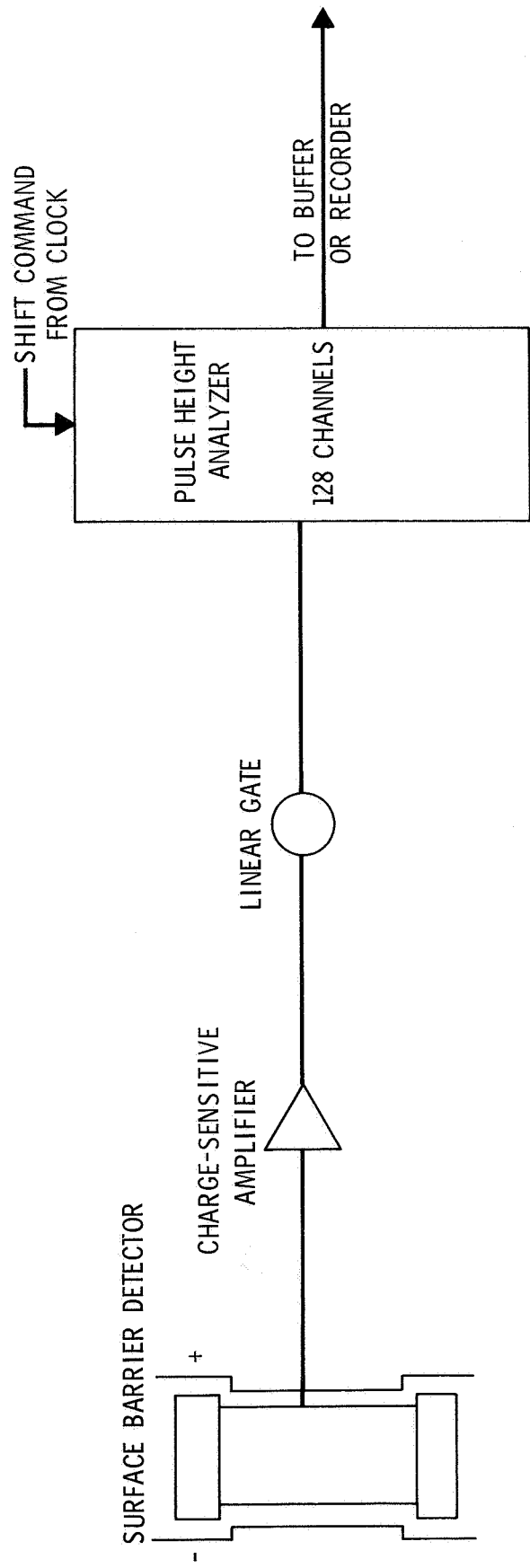


Fig. 6 Alpha Particle Monitoring System

Neutron Albedo Experiment

Ligenfelter, Canfield, and Hess⁷ have published detailed calculations on the cosmic-ray-induced leakage spectrum for several model compositions. The results show a variation with mineral type and a strong sensitivity to hydrogen content. Fig. 7, taken from the paper of Ligenfelter *et al.*, shows the expected leakage for several compositions including, for chondritic material, two different values of H/Si atomic ratios.

The accuracy of the H/Si absolute measurement is limited by two factors:

1. The statistical precision with which the ratio of slow-to-fast neutrons can be determined.

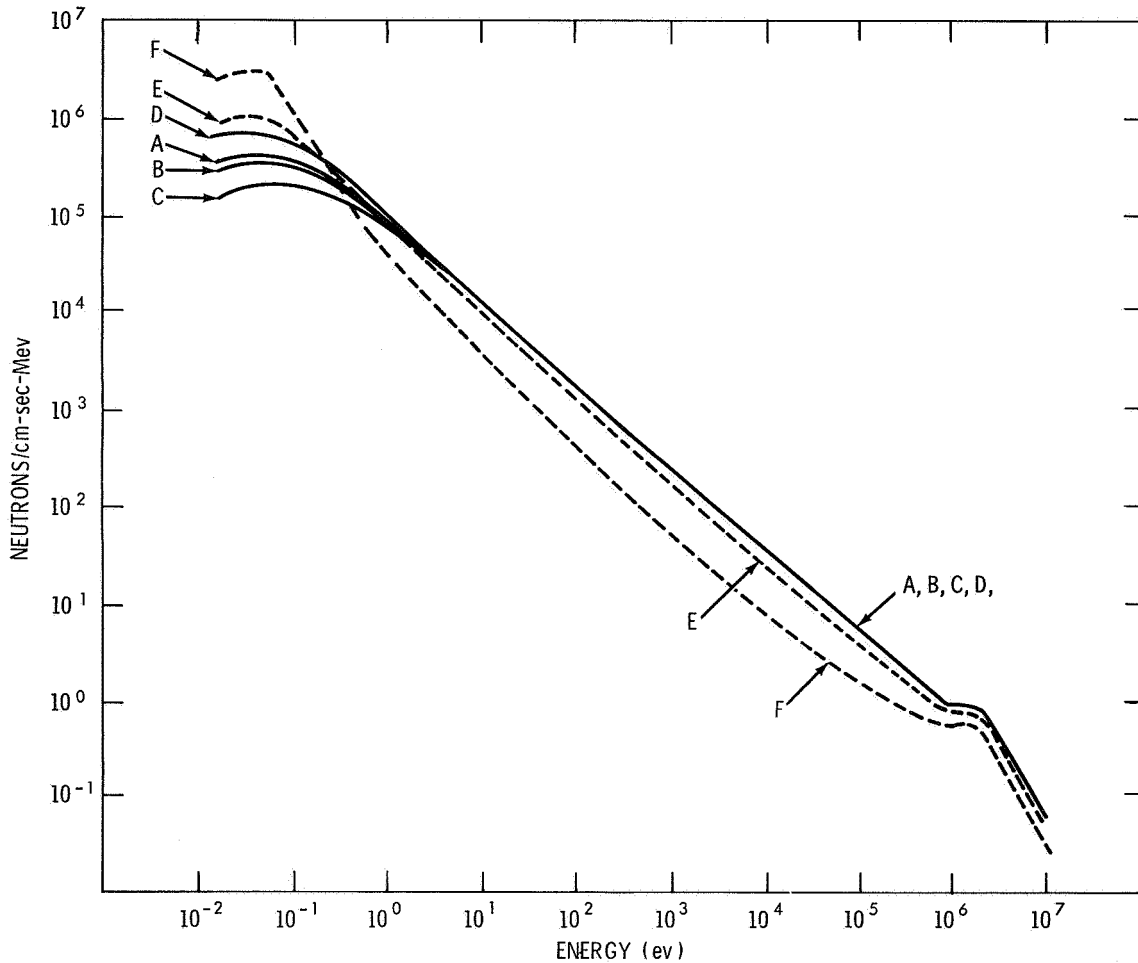


Fig. 7 Expected Neutron Leakage for Several Soil Compositions

2. The accuracy with which the thermal neutron macroscopic absorption cross-section is known. This second factor depends on a knowledge of the lunar surface composition, particularly the concentration of such elements as iron because of the very strong absorption. This information should be supplied by the gamma and X-ray measurements.

Ligenfelter et al. have calculated that hydrogen may be detected by a neutron albedo measurement if the H/Si ratio is 0.05 or greater. The atomic ratio in chondrites where water is approximately 0.3 percent by weight is approximately 0.05. In granite, one finds H/Si ratios of approximately 0.1 — twice the minimum detectable ratio.

From present estimates, statistical limitations do not seriously affect the accuracy of the H/Si determination. The relatively high neutron fluxes expected should allow the measurement of slow/fast neutron ratios to approximately ± 10 percent in 30 seconds of sampling time. For H/Si ratios of approximately 0.1, this would only contribute an approximate 10-percent uncertainty to the ratio.

The problem of thermal neutron absorption cross-section of the surface material is more serious. For example, if a ± 20 -percent uncertainty in cross-section exists, then the H/Si ratio of 0.1 can only be known to approximately ± 30 percent.

In order to perform the previously described measurement, one requires detectors for slow and fast neutrons. Two unmoderated proportional counters filled with BF_3 are proposed for detecting the slow neutrons. These two counters are identical except for ratios of B^{10} to B^{11} . One tube contains 96-percent B^{10} , and the second tube uses 10-percent B^{10} and 90-percent B^{11} . The B^{11} isotope does not react appreciably with neutrons; the B^{10} undergoes a (n,α) reaction, forming Li. The reaction has a $1/v$ dependence, where v is the neutron velocity, hence the high sensitivity to slow neutrons. The method consists of comparing the difference in counting rates between the two detectors and solving the simple simultaneous equations

$$A = 0.96n + b$$

$$A = 0.10n + b,$$

where A and B are the respective count rates, b the backgrounds, and n is related to the density of the slow neutrons.

The fast neutrons are detected through the (n, p) elastic scattering process. A special, organic scintillator sensitive to neutrons, is coupled to a photomultiplier. The readout system may consist of a simple multi-channel analyzer, although in this instance one would use the analyzer described earlier. In order to eliminate charged particles such as cosmic rays and gamma rays, an inorganic scintillator is used in the anticoincidence mode. A block diagram is shown in Fig. 8.

INTERDEPENDENCE OF MEASUREMENTS

The consideration of an integrated experiment must allow for the interaction of individual measurements. If the experimental results are correct then, in general, there should be good agreement concerning the elemental abundances where an overlap exists. Fig. 9 shows the interrelationship. Indicated are: the principal results, the data required from one experiment needed for the correct interpretation of the results of another, and those measurements needed for background corrections.

For example, consistency should be more clearly evident in the conclusions about the types of rocks being observed. Basaltic characteristics should be reflected both in low gamma activity and by higher Mg/Si ratios observed in the X-ray measurements.

Over some portions of the moon, one may observe marked disagreements because of the difference in sampling depths. Certainly some events or processes may affect the surface to micron depths measured by the X-rays, whereas the sampling depth of the gamma-ray technique is in the order of decimeters. This difference may reveal the time scale of the processes involved. If positive results obtained in the alpha particle measurements validate the radon diffusion mechanism, then one would expect enhanced gamma-ray activities at certain energies that are higher than warranted by the composition.

The largest background in the neutron experiment will be gamma-rays from the moon and the spacecraft; they will be measured as neutrons. The gamma-ray measurements will determine the flux from both these sources. On the other

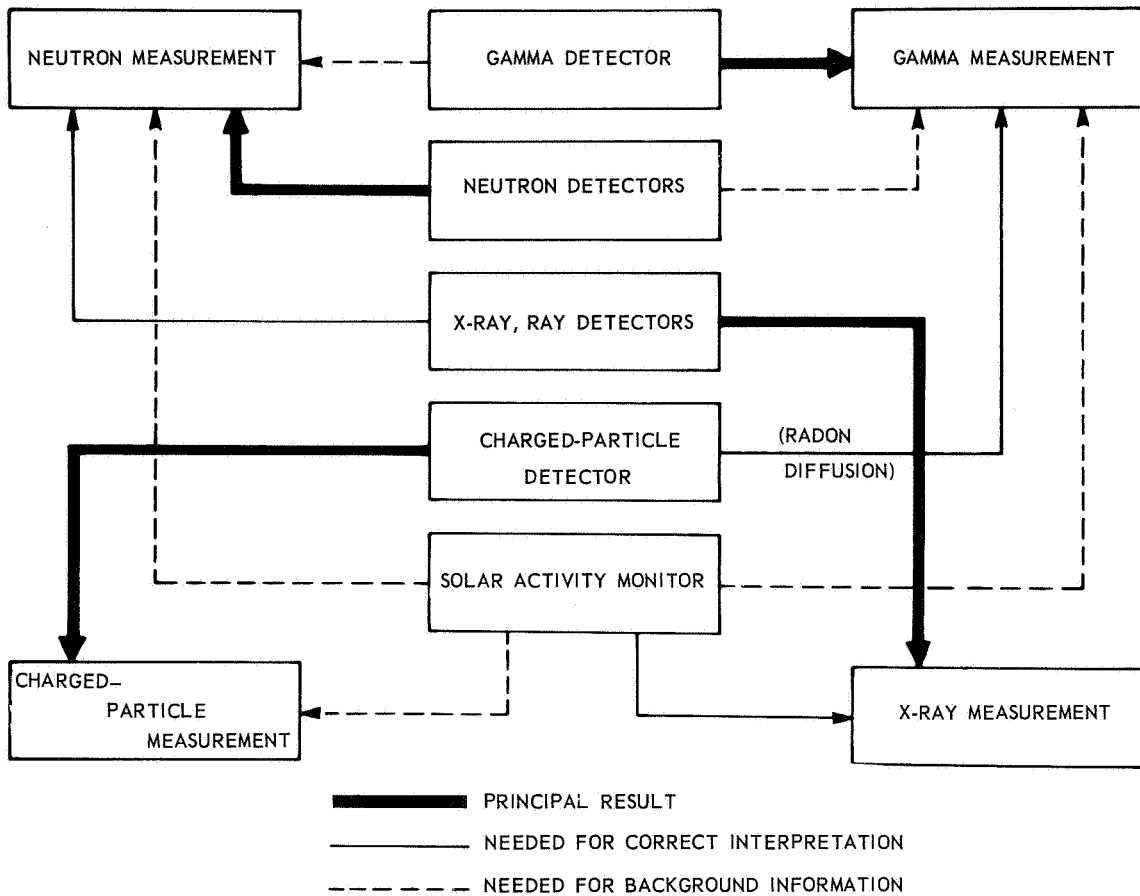


Fig. 9 Interdependence of Radiation Detector Experiments in Terms of Chemical Compositional Analysis

hand, neutron-induced events can constitute a significant portion of the background in the gamma-ray measurements.

Interpretation of the neutron albedo experiment depends largely on the concentration of certain elements in the lunar surface. For example, the most important abundance for determining the thermal neutron cross-section is that of Fe, which one hopes to obtain from the X-ray and possibly the gamma-ray experiment.

Finally, all the measurements will have about the same spatial resolution and view direction. Thus, one aspect solution should be sufficient for all measurements. In the event of uncertainty about lunar coordinates, there would be no doubt that the view directions of all the detectors were the same.

POSSIBLE MISSION FOR GEOCHEMICAL REMOTE SENSING EXPERIMENT

The foregoing discussion concerned the instrument packages; this portion of the paper will briefly consider a possible mission in which a remote sensing package might be included. Both manned and unmanned missions have been considered; that is, a directly launched Lunar Orbiter or AIMP, the use of subsatellites during an Apollo mission, and finally the inclusion of the geochemical remote sensing package in the first sector of the Command Service Module. All are likely candidates, however, size, weight, mission duration, and command and data transmission capability will determine the nature and sophistication of the package.

Let us briefly consider the configuration required for a Lunar Orbiter mission. Table 2 lists the pertinent spacecraft characteristics of a Lunar Orbiter vehicle, and Figs. 10 and 11 show a possible experiment package. The basic configuration

Table 2

LUNAR ORBITER SPACECRAFT CHARACTERISTICS

Function	Lunar Orbiter, (I-V) Boeing S/C prime Booster: Atlas-Agena D
Communications	50 bps for performance TEL, 400-mw xmtr, using omni-direct antenna (low gain); beam-width 60° about x-z plane (earth-moon); second antenna dish type for video, 10° solid angle, 10 watt xmtr; ant. steerable about boom axis only (Y) in 1° increments; L.O.S. moves in xz plane; video: 250kHz bw; removing photo subsystem and redundant measurements yields 304 bits available for science experiments, and still fit within L.O. standard frame
Propulsion-orbit change capability	1000 meters/sec total AV capability; restart capability; propellant is used for cis-lunar mid-course corrections, deboosting into lunar orbit, and various orbit inclination, and phasing changes; 100-lb thrust engine, 700 secs operation total, approx.; this capability sufficient to transfer from equatorial orbit to 35° inclination only at moon

Table 2 (Continued)

Prime power	26.6 to 31 volts on solar cells; 22 to 27 vdc on standby battery, 12 AH; depth of discharge must not exceed 40%; array delivers avg of 300 watts to present S/C system; orbit sun/shadow ratio must be \approx 4:1 or larger
Power allotted to experiments	100 watts
Attitude stabilization and control	Locks on sun in pitch and yaw using sun sensors; stabilizes in roll by sensing Canopus; 3-axis gyro stabilizes (IRU) when sun or Canopus not visible; attitude-oriented to point down over target 0.2° of local vertical; has power cap, for 3-axis maneuver every 1.2 hour, 30 days, or low activity for 11 months; orbiter team has demonstrated capability in finding and using other celestial sources for references in space over a year
Command capability	Command word 26 bits long; flight programmer (or computer) can store 128 words (21 bits each); reserved for telemetry, 8-20 bit word storage; computer can issue 120 commands; photo subsystem takes 27 commands, at 20 bits each from storage; 6 other operational codes are available, at 15 commands/code
Weight, volume available	Total S/C, 850 lbs; Photo subsystem 150 lbs; when removed, will yield experiment space of $30'' \times 30'' \times 20''$ high, approx
Antenna	1 Low-gain omni, 1 high-gain dish, 10° solid angle
On-board data storage	See flight programmer above
Typical experiments	None; spacecraft designed to carry a 150-lb photographic subsystem
Lifetime	1 year, with moderate use of propellants
Temperature control	Passive, experiments are protected; temp. range 100° F to -12° F

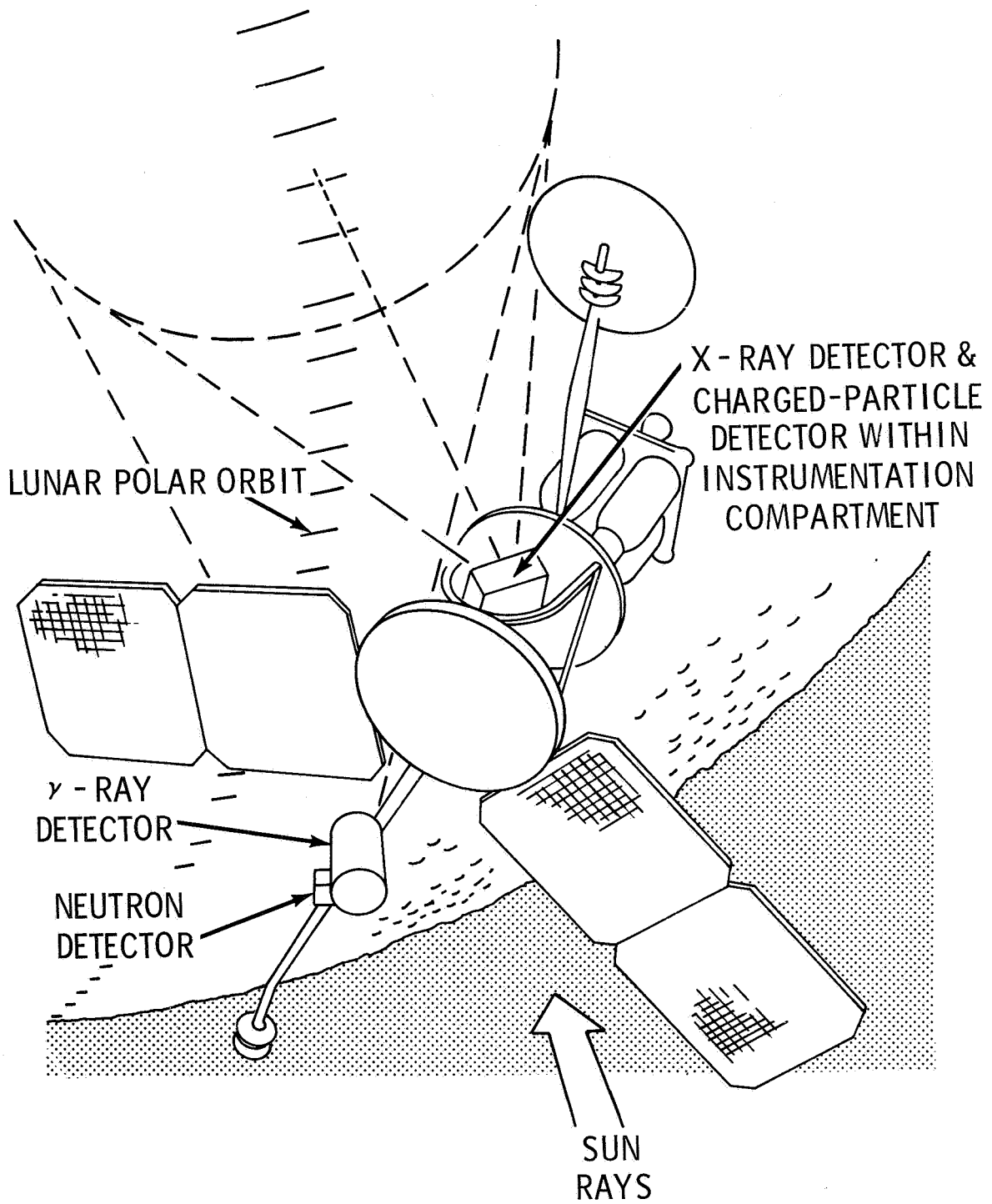


Fig. 10 Conceptual View of Radiation Detector Remote Sensing Package
Aboard Lunar Orbiter Vehicle

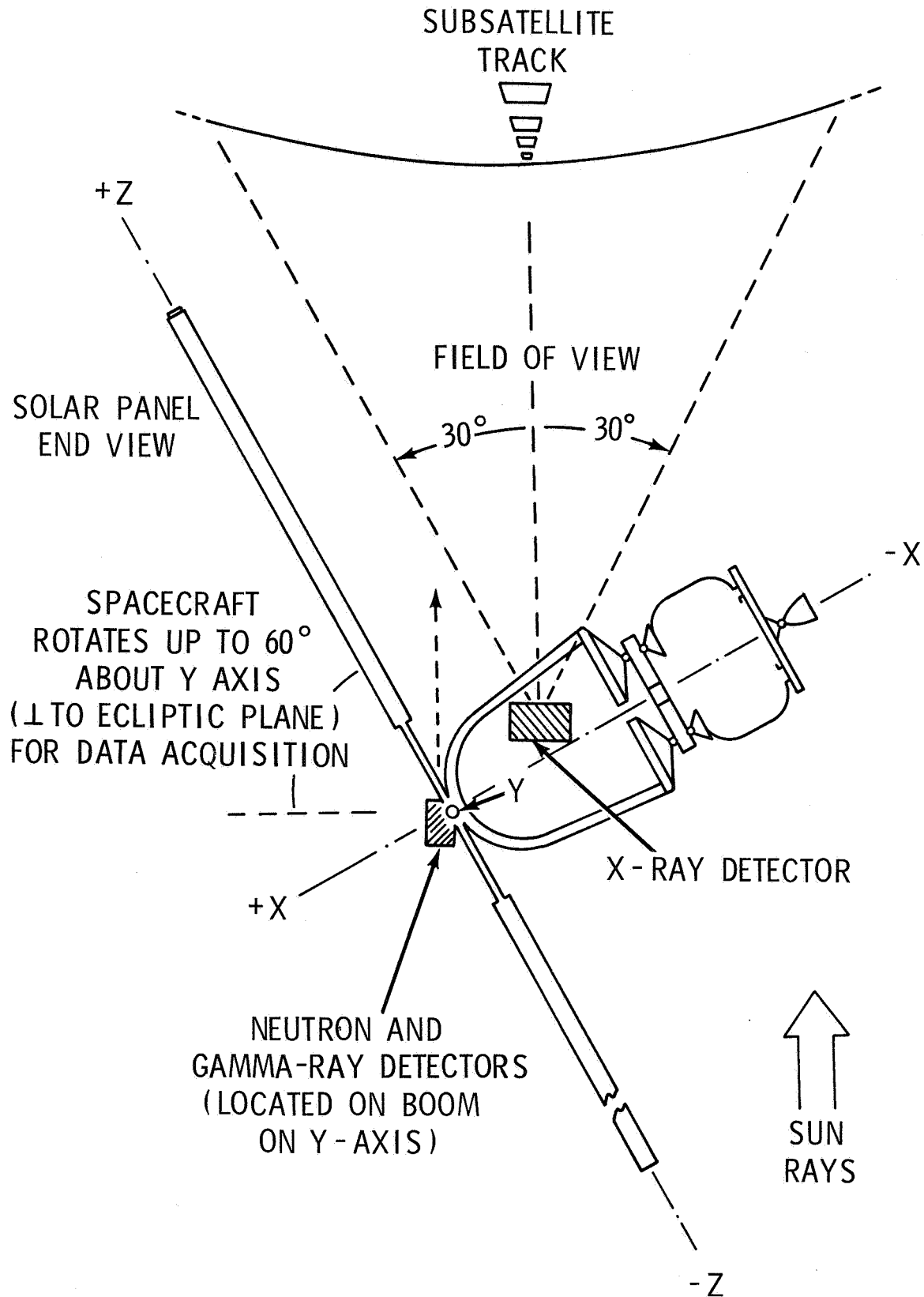


Fig. 11 Plan View of Lunar Orbiting Satellite

involves one group of detectors mounted within the body of the spacecraft with a view of the surface and other instruments mounted on a boom. Assuming that the detector is nominally pointed down, the instantaneous view area on the moon (area of moon from which radiation can reach the detector) is a function of the detector field of view and the altitude of the spacecraft above the lunar surface (Fig. 12). Another relevant factor is the time required for the detector to traverse the view area. In a near-moon orbit, the orbital velocity will be approximately 1.7 km/sec; thus, in 30 seconds, the detectors will sweep a 50-km swath of the moon's surface. This is comparable to the diameter of the view area if the satellite is 50 km above the surface for a detector with a ± 30 -degree field of view.

The detectors can be made to view the surface continuously only if the satellite or detector can be made to point toward the center of the moon. In general, the spacecraft axes will be fixed in inertial space, and the moon surface will be viewed only during a portion of the orbit as shown in Fig. 13 where the area ABCD comprises the portion of the surface "seen" during a single pass. During other times, if the spacecraft is in a fixed inertial mode and if the detectors are not pivoted, the detectors will view open space. From one orbit to the next, different segments of the moon will be viewed because of the rotation of the moon about its axis.

ACKNOWLEDGMENTS

The authors gratefully acknowledge Dr. J. Arnold, University of California, San Diego; Dr. A. Metzger, Jet Propulsion Laboratory; Dr. J. Carpenter, Dr. H. Gersky, and Dr. P. Gorenstein of American Science and Technology; and J. Frisora, G. Streeter, and T. Rizzo, GSFC; for their help and permission to use some of the materials contained in this paper.

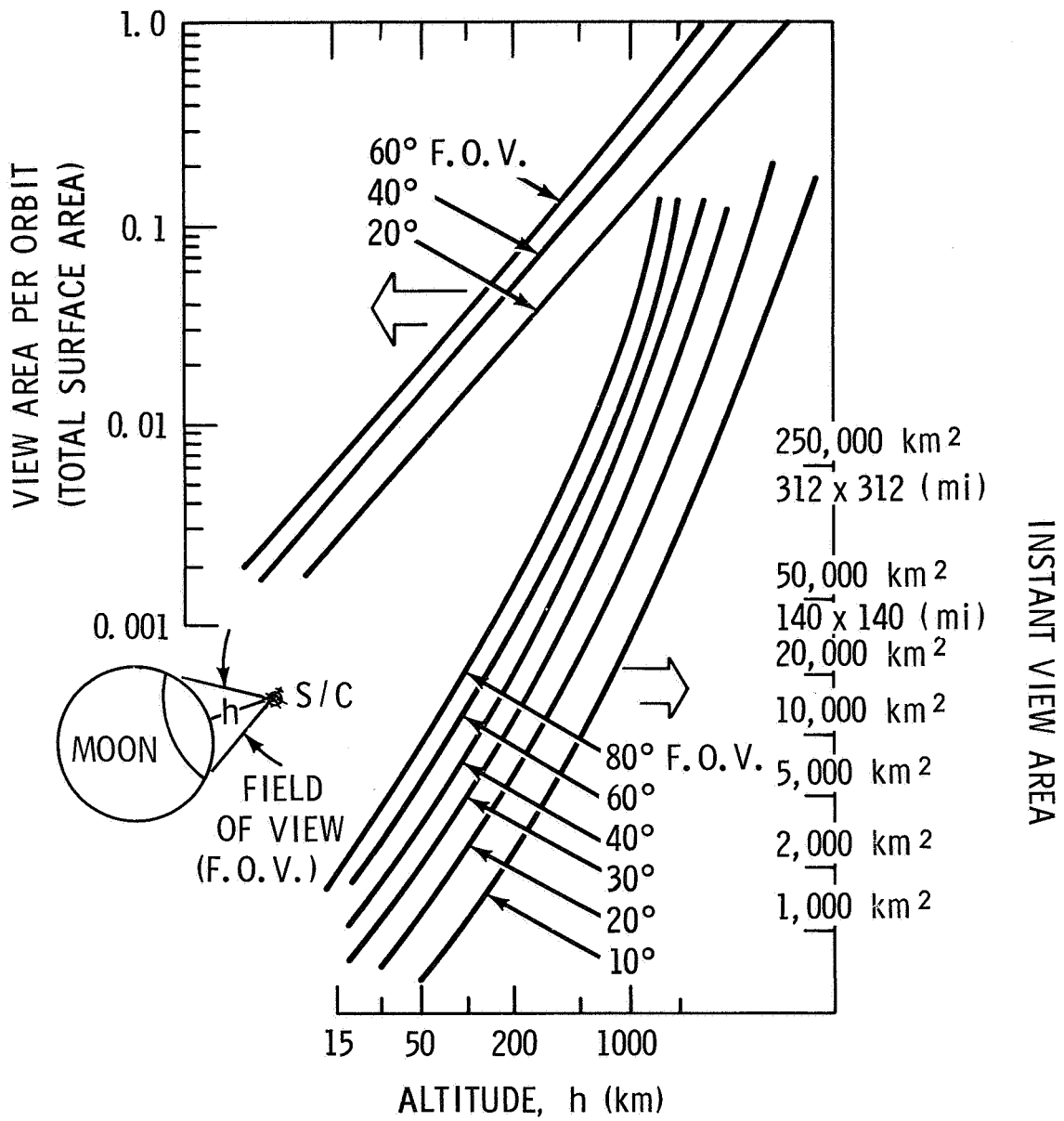


Fig. 12 View Area Parameters

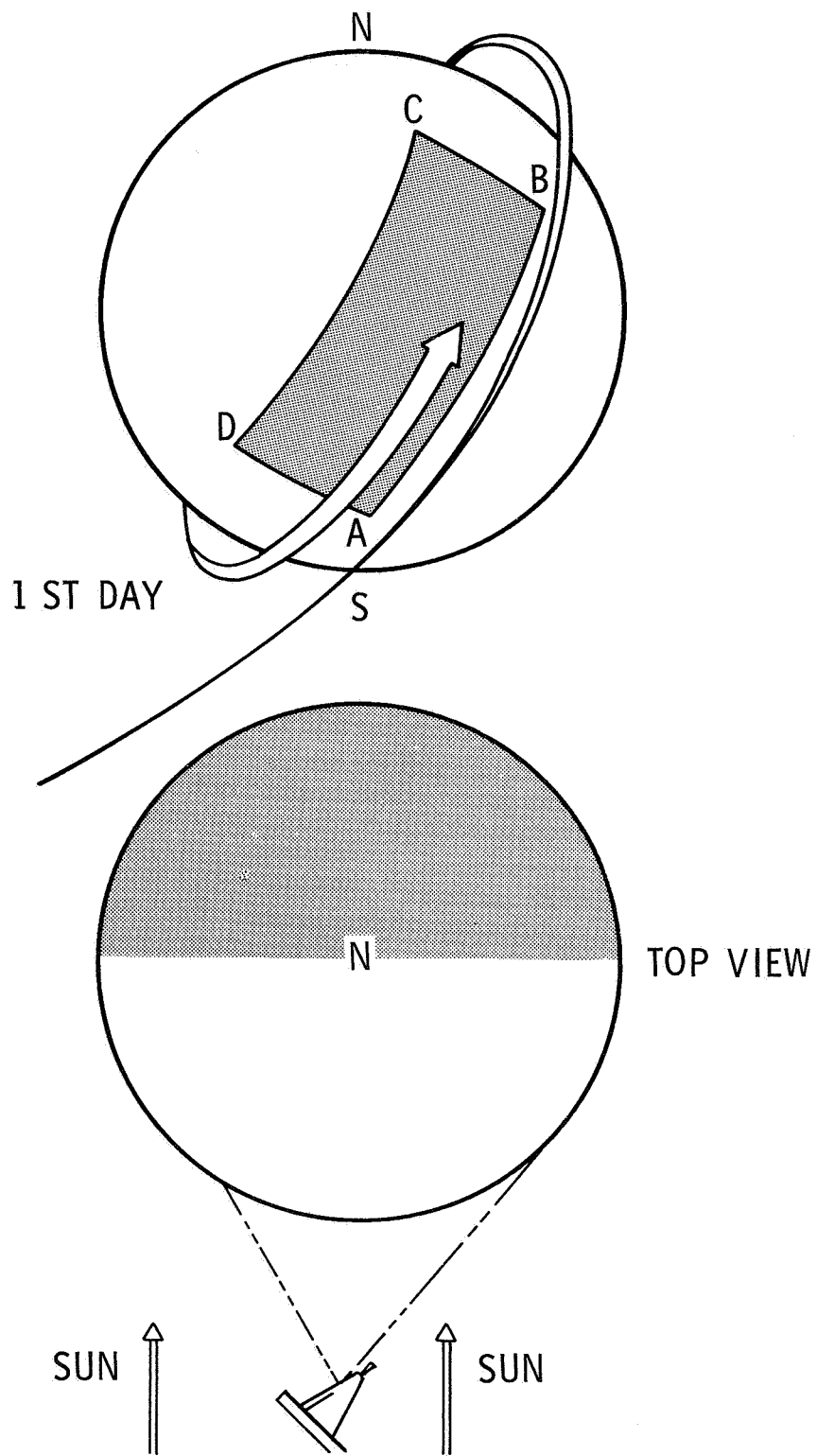


Fig. 13 Scan Area for Equator-Polar Orbit

REFERENCES

1. A. Turkevitch, E. Franzgrote, and J. H. Patterson, Science 631, Nov. 3, 1967
2. A. P. Vinogradov, Yu. A. Surkov, G. M. Chernov, F. F. Kirnozov, and G. B. Nazarkiva, "Gamma Investigation of the Moon and Composition of the Lunar Rocks," tenth meeting of COSPAR, London, 1967
3. J. Carpenter, P. Gorenstein, H. Gursky, B. Harris, J. Jordan, T. McCallum, M. Ortman, L. Sodickson, "Final Report, Lunar Exploration by Satellite," ASE-1919, American Science and Engineering, Cambridge, Mass.
4. J. Arnold, Private Communication
5. T. W. Armstrong and R. G. Alsmiller, Jr., Personal Communications
6. H. W. Kraner, G. L. Schroeder, G. Davidson, and J. W. Carpenter, Science, 152, 1235, 1966
7. R. E. Ligenfelter, E. H. Canfield, and W. N. Hess, J.G.R. 66, 2665, 1961